



# Impaired bone microarchitecture in distal interphalangeal joints in patients with primary hypertrophic osteoarthropathy assessed by high-resolution peripheral quantitative computed tomography

Q. Pang<sup>1,2</sup> · Y. Xu<sup>1,3</sup> · X. Qi<sup>1</sup> · L. Huang<sup>2</sup> · V.W. Hung<sup>2</sup> · J. Xu<sup>2</sup> · R. Liao<sup>1</sup> · Y. Hou<sup>1</sup> · Y. Jiang<sup>1</sup> · W. Yu<sup>4</sup> · O. Wang<sup>1</sup> · M. Li<sup>1</sup> · X. Xing<sup>1</sup> · W. Xia<sup>1</sup> · L. Qin<sup>2</sup>

Received: 13 March 2019 / Accepted: 12 September 2019 / Published online: 23 October 2019  
© International Osteoporosis Foundation and National Osteoporosis Foundation 2019

## Abstract

**Summary** This study aimed to investigate the bone impairment in finger joints in PHO patients by HR-pQCT. Results showed distinguished differences in bone architecture and biomechanics parameters at DIPs between PHO patients and healthy controls using HR-pQCT assessment. Besides, serum PGE2, hsCRP and ESR levels were found negatively correlated with total vBMD.

**Introduction** This study aimed to investigate the bone impairment in finger joints in primary hypertrophic osteoarthropathy (PHO) patients firstly by high-resolution peripheral quantitative computed tomography (HR-pQCT).

**Methods** Fifteen PHO patients and 15 healthy controls were enrolled in this study. Bone erosions in hands at distal interphalangeal joints (DIPs) in both PHO patients and controls were evaluated by X-ray. Bone geometry, vBMD, microstructure parameters, and size of individual bone erosion were also measured at the 3rd DIP by HR-pQCT as well. Blood biochemistry levels between the two groups were also compared.

**Results** Compared to X-ray, HR-pQCT assessment were more sensitive for detection of bone erosions, with 14 PHO patients by HR-pQCT versus ten PHO patients by X-ray judged at the 3rd DIP. The average depth, width, and volume of erosions size in PHO patients were  $1.38 \pm 0.80$  mm,  $0.79 \pm 0.27$  mm, and  $1.71 \pm 0.52$  mm<sup>3</sup>, respectively. The bone cross-areas including total area (+ 25.3%,  $p \leq 0.05$ ), trabecular area (+ 56.2%,  $p \leq 0.05$ ), and cortical perimeter (+ 10.7%,  $p \leq 0.05$ ) at the defined region of interest of 3rd DIP was significantly larger than controls. Total vBMD was 11.9% lower in PHO patients compared with the controls ( $p \leq 0.05$ ). Biochemical test results showed the increased levels of inflammatory cytokines, bone resorption markers, and joint degeneration markers in PHO patients. Serum prostaglandin PGE2, high-sensitive C-reactive protein (hsCRP) and erythrocyte sedimentation rate (ESR) levels were found negatively correlated with total vBMD.

**Conclusions** This study demonstrated higher sensitivity of the HR-pQCT measurement at DIPs by showing the differences in architecture and biomechanics parameters at DIPs between the PHO patients and healthy controls, which would be of interest clinically to investigate bone deterioration in PHO patients.

**Keywords** Distal interphalangeal joints · HR-pQCT · Primary hypertrophic osteoarthropathy · Prostaglandin PGE2

---

**Electronic supplementary material** The online version of this article (<https://doi.org/10.1007/s00198-019-05168-3>) contains supplementary material, which is available to authorized users.

---

✉ W. Xia  
xiaweibo8301@163.com

✉ L. Qin  
lingqin@cuhk.edu.hk

Extended author information available on the last page of the article

## Introduction

Primary hypertrophic osteoarthropathy (PHO) is a genetically and clinically heterogeneous disease characterized by pachydermia, digital clubbing (swelling of the soft connect tissue), and skeletal abnormalities consisting of periostosis of long bones and acro-osteolysis of distal phalanges of fingers and toes [1]. The underlying pathogenesis of PHO is reported as the increased levels of prostaglandin PGE2 due to dysfunction of PGE2 metabolism pathway caused by

homozygous or heterozygous mutations of *HPGD* (MIM 601688) or *SLCO2A1* (MIM 601460) which encodes the major PGE2 catabolizing enzyme (15-hydroxyprostaglandin dehydrogenase, 15-PGDH) or a prostaglandin transporter protein [2, 3]. This results in autosomal recessive primary hypertrophic osteoarthropathy 1 (PHOAR1) and autosomal recessive primary hypertrophic osteoarthropathy 2 (PHOAR2) respectively [2, 3]. PGE2 acts in an autocrine or paracrine manner and initiates various signaling pathway upon binding to its receptors (EP1~EP4) in different tissues [4]. Higher PGE2 has been associated with a wide range of pathological conditions [5]. Biochemical assessment of PHO patients showed elevated levels of PGE2 in both forms of PHO (PHOAR1 and PHOAR2) [2–4, 6].

PHO closely mimics hypertrophic osteoarthropathy (HOA) secondary to pulmonary or other systematic diseases. Arthritis is often the presenting complaint in HOA. The joint involvement in HOA is commonly characterized radiologically by the presence of synovial effusion [5]. PGE2 plays a crucial role in the pathogenesis of osteoarthritis (OA) and rheumatoid arthritis (RA) through coupling to its receptors (EP2 and EP4) and regulating the immune response [7, 8]. The increased levels of PGE2 have been reported in synovial fluid and cartilage from patients with OA and RA [7–9]. In the PHO study, arthritic diseases such as arthralgia and arthritis presented in 20–40% PHO patients with affecting mainly at knees, ankles, and wrists [1]. This indicated that joint symptoms were another common triads in PHO patients. Additionally, almost all of the reported PHO patients were under inflammatory conditions with elevated levels of high sensitive C-reactive protein (hsCRP) and erythrocyte sedimentation rate (ESR) which have been demonstrated positively correlated with PGE2 levels with typical inflammatory syndromes including joint and soft-tissue swelling and pains [4, 10]. Besides, a reported PHO case has also shown an increased level of interleukin 6 (IL-6) [11]. Histologically, bone biopsy showed inflammatory reaction in the periosteum [12]. These results indicated that PHO might be a chronic inflammatory disease associated with joint deterioration apart from the classical skeletal and tissue manifestations. Inflammation at the joints which induced secondary osteoporosis and bone erosions has been well recognized in RA, which was also a chronic immune-mediated destructive arthritis characterized by chronic inflammatory synovitis and bone loss. Redlich *et al.* [13] revealed that excessive production of inflammatory cytokines influenced bone metabolism by enhancing osteoclast activity and inhibiting osteoblast function, resulting in progressive bone loss. In previous PHO radiographic studies, acro-osteolysis of the distal phalanges of fingers and toes and periosteal thickening along the diaphysis of the long bone were commonly observed by X-ray examination [2–4, 10], whereas reports on evaluation of bone erosions or bone loss related to joint damage development in PHO patients were still lacking.

Traditionally, the presence of bone erosions is evaluated by conventional radiography (X-ray) at the joints of hands or feet. However, 2D plane X-ray is limited by its sensitivity in the detection of erosions as compared with magnetic resonance imaging (MRI) or high-resolution peripheral quantitative (HR-pQCT) [14–16]. HR-pQCT is a 3D imaging technique specifically developed for *in vivo* quantitative evaluation of human peripheral skeleton at the microscale level [15]. Comparative studies have demonstrated that HR-pQCT was more sensitive than MRI and X-ray in the detection of erosions in finger joints [17, 18]. Moreover, HR-pQCT allows separating measurement of cortical and trabecular volumetric bone mineral density (vBMD) and bone microstructures in finger joints [19].

In the current study, HR-pQCT was used to image the distal interphalangeal joints (DIPs) in both PHO patients and healthy controls. We hypothesized that HR-pQCT could detect accurately the bone deterioration and erosion caused by persistent inflammation in PHO patients at DIP sites. Thus, the aims of this study were to (1) use HR-pQCT to investigate bone impairment in finger joints in PHO patients who sought for medical advice for the first time and did not receive any anti-osteoarthritis, anti-bone resorption, and prostaglandin synthase-2 (COX-2) selective inhibitor treatment, including for the first time evaluation of bone geometry, vBMD, microstructure, biomechanical parameters, and quantification of bone erosions at DIP; and (2) assess the clinical risk factors or biochemical indices, including serum levels of PGE2, inflammatory cytokines, bone metabolic markers, and cartilage degeneration markers which influence cortical and trabecular vBMD, microstructure, and biomechanical at the DIP site in patients with PHO.

## Methods and materials

### Subjects

Sixteen patients with PHO from the Endocrinology Outpatient Clinic of the Peking Union Medical College Hospital (PUMCH) were recruited from May 2016 to November 2017. All patients fulfilled the clinical, radiological, and genetic criteria for PHO, which included (1) clinical presentation of digital clubbing, pachydermia, and palmar and plantar hyperhidrosis; (2) X-ray finding of periostosis; and (3) *HPGD* or *SLCO2A1* mutation confirmation. After initial recruitment, all PHO patients were screened to exclude those who (1) had the history of other metabolic disorders; (2) used corticosteroid, nonsteroidal anti-inflammatory drugs (NSAIDs), and pamidronate in 6 months; (3) received anti-bone resorption medications, such as bisphosphonate and teriparatide in a year; and (4) underwent treatment with bone active drugs, such as hormonal therapy, thyroxine, and thiazide diuretic.

Only one PHO patient was excluded from the present study as he had received Diclofenac sodium extended-release tablets, known as a nonsteroidal anti-inflammatory drug, for 1 month before entered the project. Altogether, 15 PHO patients fulfilled inclusion and exclusion criteria and were enrolled in this study. Additionally, age-, gender-, and ethnicity-matched 15 unrelated healthy individuals from physical examination center of PUMCH were studied as healthy controls. All eligible healthy controls must fulfill the following criteria: (1) no carrying *HPGD* or *SLCO2A1* mutations; (2) no suffering from hand-joint complaints or other joints complaints; (3) no history of bone fractures; and (4) no receiving any anti-bone resorption drugs, bone active drugs, and NSAIDs in a year before entering the study. All enrolled patients and healthy controls underwent X-ray screening on both hands and HR-pQCT examinations on the non-dominant hand and biochemical assessments. Based on the HR-pQCT images, the erosion size was measured. All subjects signed informed consent for imaging measures as well as blood sample collections. This study was approved by the Ethics Committee of PUMCH with the ethics audit number zs-1115.

### X-ray acquisition and erosion scoring

X-ray images of both hands with palmar surface in contact with the cassette and the fingers slightly spread were obtained from each study individual in the Department of Radiology of PUMCH. During the scanning process, the hands were placed on the same film-containing plate to avoid development variation. The double-blind grading was performed to grade the bone erosions from radiographs of hands by two experienced readers with reference to the Atlas of Standard Radiographs of Arthritis [20]. The scores were analyzed by two trained observers twice with a 2-week interval for intra- and inter-reader reliability.

Individual radiographic features were recorded for eight joints of each hand including four distal interphalangeal (2nd–5th DIP) and four proximal interphalangeal (2nd–5th PIP) joints. The erosion of each joint was graded as 1 or 0 with the presence or not of erosion, respectively. For assessment of intra- and inter-reliability of X-ray erosion measures, the erosions grading with the X-ray images were evaluated by two trained readers. Firstly, the X-ray images were evaluated by single trained reader. Two weeks later, these same measurements were retaken to ascertain intra-reader reliability using the intraclass correlation coefficient (ICC). Meanwhile, using the same X-ray images, inter-reader reliability was examined by two trained readers.

### HR-pQCT image acquisition

Bone loss at the DIP of the non-dominant hand was examined by HR-pQCT (Xtreme CT II, Scanco Medical AG, Brüttisellen, Switzerland) by using the standard protocol

with 68 kVp tube voltage, 1470  $\mu$ A tube current and 91  $\mu$ m isotropic voxel size. For the DIP acquisition, the subject's forearm was fixed in a palm-down orientation within a custom carbon-fiber cast designed at our institution [21]. The assessment was confined to the DIP region to optimize time efficiency and minimize motion artefact. The region of interest (ROI) was defined as the top of the 3rd DIP, such that the scan region with 6.5 mm in proximal direction and 19.9 mm in distal direction (total scan length was 26.4 mm, 290 slices). We chose an effective ROI for 3rd DIP head analysis of 67 slices corresponding to approximately 6.5 mm in the axial direction (Supplementary Figure 1). The total scan time was 6.3 min with an effective radiation dose of approximately 5  $\mu$ Sv.

### Bone erosion evaluation based on HR-pQCT images

For bone erosion analysis, the palmar, ulnar, dorsal, and radial quadrants at the base of the 3rd DIP were evaluated on a PACS workstation using the open source Digital Imaging and Communication in Medicine (DICOM) OsiriX software (OsiriX MD 10.0; download from [www.osirix-viewer.com](http://www.osirix-viewer.com)). Erosions were defined as sharply marginated bone lesions with juxta-articular location with a cortical break seen in at least two adjacent slices as described previously [18]. According to Finzel's study [22], pseudo-erosions, resulting from marginal osteophytes, were recognized and excluded from further assessment. All parameters of bone erosions including the erosion width, depth, and volume were analyzed twice with a 2-week interval [19, 21, 23]. The maximum depth of each erosion was recorded using electronic calipers on axial images. The maximum width was recorded using electronic calipers either on the axial plane or reformatted sagittal or coronal plane images. The volume of erosion was assessed using a semi-automated method. The area of erosion was determined by defining the entire area of the distal phalangeal bone on each image of the erosion (A1) or excluding erosion (A2). The volume ( $V_{\text{erosion}}$ ) of the erosion was calculated as  $V_{\text{erosion}} = (A1 - A2) \times n \times 0.091$ , where  $n$  is the total number of slice with the erosions and 0.091 is the height of the slice [19]. For assessment of intra- and inter-reader reliability of erosion size, the erosion width, depth, and volume were firstly evaluated by a single trained reader. The same assessments were performed to ascertain intra-reader reliability using ICC. The inter-reader reliability was performed based on the same set of image data by two trained readers.

### HR-pQCT parameters assessment

The trabecular and cortical evaluation protocols were used to evaluate the bone geometry, bone quality, and bone microstructure as described in published studies [24–26]. Five parameters were obtained for bone geometry evaluation, including total bone area (Tt.Ar,  $\text{mm}^2$ ), cortical bone area (Ct.Ar,

mm<sup>2</sup>), trabecular bone area (Tb.Ar, mm<sup>2</sup>), cortical perimeter (Ct.Pm, mm), and cross-sectional moment of inertia (CSMI, mm<sup>4</sup>). The total vBMD (Tt.vBMD), trabecular vBMD (Tb.vBMD), and cortical vBMD (Ct.vBMD) were obtained for bone quality evaluation. The bone microarchitecture was evaluated by the following parameters: trabecular bone fraction (Tb.BV/TV), trabecular number (Tb.N, 1/mm), trabecular thickness (Tb.Th, mm), trabecular separation (Tb.Sp, mm), cortical thickness (Ct.Th, mm), and cortical porosity (Ct.Po, %). Bone strength index (BSI) was used for estimation of bone strength and was determined using following published equation [27]:  $BSI = CSMI \text{ (mm}^4\text{)} \times \text{volumetric cortical BMD (mg HA/cm}^3\text{)}$ .

## Biochemistry

Fasting morning blood samples were collected from all participants at the same day of imaging. The blood samples were centrifuged at 3000 r/min under 4 °C for 10 min to obtain the serum for biochemical analysis. The following biochemical markers were assessed at the central laboratory of PUMCH: (1) inflammatory index: hsCRP, ESR, IL-6, and tumor necrosis factor alpha (TNF- $\alpha$ ) by standard methods; (2) serum PGE2 by competitive enzyme-linked immunosorbent assays (ELISA) according to the manufacturer's protocol (Cayman Chemicals, Ann Arbor, Michigan, USA); (3) markers of bone metabolism: alkaline phosphatase (ALP) by standard methods, intact parathyroid hormone (iPTH), and beta-C-telopeptides of type I collagen ( $\beta$ -CTX) by an automated Roche electrochemiluminescence system (E170 Roche Diagnostics, Basel, Switzerland), free soluble receptor activator of nuclear factor-kappa B Ligand (sRANKL) and osteoprotegerin (OPG) by sandwich ELISAs according the manufacturer's protocol (Biovendor, Czech); and (4) markers of cartilage degeneration: matrix metalloproteinase-1 (MMP1) and matrix metalloproteinase-13 (MMP13) by sandwich ELISAs according the manufacturer's protocol (Abcam, UK).

## Statistical analysis

Kolmogorow-Smirnov test was used to test the normality of continuous variables. Normally distributed data (ALP, iPTH, Free sRANKL/OPG,  $\beta$ -CTX, hsCRP, ESR, TNF- $\alpha$ , IL-6, MMP1, MMP13, bone geometry, volumetric bone density, microstructure parameters, BSI, and erosion size) were expressed as the means  $\pm$  standard deviation (SD). Non-normally data included serum PGE<sub>2</sub>, trabecular separation, and cortical porosity were expressed as medians interquartile range. The Mann-Whitney *U* test or Student's *t* test was used to compare the difference between PHO patients and healthy controls on biochemistry, bone geometry, vBMD, and microstructure parameters. The correlation between the HR-pQCT parameters and the biochemical markers was studied using

Pearson's rank or Spearman's rank correlation test, as appropriate. All hypotheses were two-tailed and  $p \leq 0.05$  was considered to be significant. Statistical analysis was performed using SPSS version 22.0 (IBM SPSS Statistics 22.0).

## Results

### Subjects characteristics

All of the 15 PHO patients enrolled in this study were males and from unrelated unconsanguineous families of Chinese Han origin. Five of the 15 patients were positive for *HPGD* mutations, and the remaining ten patients were positive for *SLCO2A1* mutations (Supplementary Table 1). The onset age of PHO patients has a bimodal distribution, peaking during puberty in PHOAR2 patients and around the first year of life in PHOAR1 patients. The clinical characteristics of the PHO patients and healthy controls are presented in Table 1. Mean age of the 15 PHO patients was  $29.6 \pm 7.57$  years, which was not significantly different with the healthy controls ( $33.8 \pm 7.21$ ,  $p = 0.180$ ).

### Assessment of hand X-ray

By X-ray examination, acro-osteolysis of the DIPs has been detected in 13/15 PHO patients. The presence or absence of bone erosions was determined based on X-ray images of finger joints in each group (2nd~5th DIP and 2nd~5th PIP) as shown in Table 2. The 3rd DIP was almost the most frequently affected in PHO patients when compared with other finger joints. Besides, in consideration of the potential metabolic or joint disease, the healthy control (C3) who had the bone erosion at 4th PIP region was excluded in this study, though the C3 had no arthritic sign or symptoms. The intra- and inter-reader agreement of bone erosions measurement in PHO patients was excellent as data presented in Table 2.

### Evaluation of erosion size based on HR-pQCT images

Sixty-seven slices scanned from the 3rd DIP were evaluated in 15 PHO patients and 15 healthy controls. Erosions were found in 14 PHO patients and three healthy controls. Three healthy controls who had erosion detected in HR-pQCT images were deemed to be false positive findings and thereby were excluded for the further HR-pQCT parameters and biochemical analysis. For the PHO patients, the mean of the erosion width, depth, and volume was  $1.38 \pm 0.80$  mm (0.40~3.44 mm),  $0.79 \pm 0.27$  mm (0.37~1.44 mm), and  $1.71 \pm 0.52$  mm<sup>3</sup> (0.73~2.75 mm<sup>3</sup>), respectively. The intra- and inter-reader agreement of the erosion width, depth, and volume measurements was excellent (Supplementary Table 2).

**Table 1** Clinical characteristics compared between PHO patients and healthy controls

Characteristics	PHO patients ( <i>n</i> = 15)	Healthy controls ( <i>n</i> = 15)
Gender (male/female)	15:0	15:0
Height (m)	1.740 ± 0.07	1.739 ± 0.07
Pachydermia	15 (100%)	–
Periostosis	15 (100%)	–
Palmar and plantar hyperhidrosis	15 (100%)	–
Digital clubbing	15 (100%)	–
Self-reported hand pain	7 (47%)	–
Hand swollen	2 (13%)	–

### Analysis of HR-pQCT parameters

HR-pQCT measurement of bone geometry, vBMD, microstructure parameters, and estimated bone strength (BSI) is summarized in Table 3. PHO patients showed significantly larger Total.Ar, Tb.Ar, and Ct.Pm (+ 25.3%, + 56.2%, and 10.7%,  $p < 0.05$ , respectively) than healthy controls. PHO patients also had greater CSMI (+ 39.1%,  $p < 0.05$ ) than healthy controls, but there was no significant difference in BSI (+ 38.8%,  $p = 0.072$ ) between PHO patients and healthy controls. The total vBMD was lower in PHO patients (– 11.9%,  $p < 0.05$ ) compared to the healthy controls. The bone microstructure parameters were comparable between PHO patients and the healthy controls except the Tb.Sp, which was significantly greater in PHO patients than healthy controls (+ 27.3%,  $p < 0.05$ ).

Correlations between cortical vBMD and the selected geometric indicators of cortical bone (Ct.Ar, Ct.Th, and CSMI) were summarized in Supplementary Figure 2. It was found that there was no significant correlation between the cortical vBMD and bone geometric parameters in the PHO patients.

### Biochemical analysis

Both serum and urinary level of biochemical markers are listed in Table 4. The median level of serum PGE<sub>2</sub> was significantly higher than that of the healthy controls (368.2 pg/ml versus 169.1 pg/ml,  $p < 0.05$ ). For bone metabolic makers, β-CTX (0.93 ± 0.42 ng/ml versus 0.40 ± 0.06 ng/ml,  $p < 0.05$ ) and free sRANKL/OPG (279.3 ± 178.2 versus 132.9 ± 72.11,  $p < 0.05$ ) were significantly higher than that of the healthy controls. The cartilage degeneration marker MMP1 (182 ± 184.3 pg/ml versus 549.1 ± 156.8 pg/ml,  $p < 0.05$ ) was significantly higher in PHO patients than that of the healthy controls.

### Association between HR-pQCT parameters and biochemical markers

The correlation between the HR-pQCT parameters and proinflammatory markers, including serum PGE<sub>2</sub>, ESR, hsCRP, IL-6 and TNF-α, is presented in Table 5. Serum PGE<sub>2</sub> ( $r = -0.5440$ ,  $p < 0.05$ ), hsCRP ( $r = -0.5824$ ,  $p < 0.05$ ), and ESR levels ( $r = -0.5683$ ,  $p < 0.05$ ) were negatively correlated with Total.vBMD. In addition, hsCRP was found negatively correlated with CSMI ( $r = -0.4989$ ,  $p < 0.05$ ) and BSI ( $r = -0.5121$ ,  $p < 0.05$ ). ESR was positively correlated with Tb.Ar ( $r = 0.5556$ ,  $p < 0.05$ ). There was no significant correlation between HR-pQCT indices, IL-6 and TNF-α. Moreover, the results also showed that there was no significant correlation among HR-pQCT parameters, bone biomarkers (ALP, iPTH, β-CTX, and free sRANKL/OPG), and cartilage degeneration markers (MMP1 and MMP13) in the PHO patients (Supplementary Table 3).

**Table 2** Radiographic bone erosions of bilateral hands for DIP and PIP joints compared between PHO patients and the healthy controls

	PHO patients (mean ± SD, <i>n</i> )	Healthy controls (mean ± SD, <i>n</i> )	Intra-reader agreement (ICC, 95%CI)	Inter-reader agreement (ICC, 95%CI)
2nd DIP	0.20 ± 0.32 ( <i>n</i> = 4)	0	0.818, 0.541–0.935	0.895, 0.717–0.964
3rd DIP	0.53 ± 0.44 ( <i>n</i> = 10)	0	0.921, 0.781–0.973	0.909, 0.750–0.968
4th DIP	0.30 ± 0.37 ( <i>n</i> = 6)	0	0.945, 0.844–0.981	0.895, 0.717–0.964
5th DIP	0.40 ± 0.43 ( <i>n</i> = 7)	0	0.904, 0.738–0.967	0.910, 0.755–0.969
2nd PIP	0.27 ± 0.32 ( <i>n</i> = 6)	0	0.904, 0.776–0.972	0.901, 0.732–0.966
3rd PIP	0.47 ± 0.44 ( <i>n</i> = 9)	0	0.926, 0.794–0.974	0.927, 0.797–0.975
4th PIP	0.40 ± 0.39 ( <i>n</i> = 8)	1, 0.03 ± 0.13	0.942, 0.837–0.980	0.896, 0.719–0.964
5th PIP	0.50 ± 0.46 ( <i>n</i> = 9)	0	0.959, 0.883–0.986	0.899, 0.727–0.965

The intra- and inter-reader agreement of bone erosions measurement in PHO patients. The most frequently affected interphalangeal joint of X-ray bone erosion evaluation was italicized

*n* number, *DIP* distal interphalangeal, *PIP* proximal interphalangeal, *ICC* intraclass correlation coefficient, *CI* confidence interval

**Table 3** Comparison of HR-pQCT parameters in PHO patients and the healthy controls

	PHO patients (n = 15)	Healthy controls (n = 12)	Difference (%)
<b>Bone geometry</b>			
Total.Ar (mm <sup>2</sup> )	51.32 ± 10.60	40.96 ± 4.07	25.3*
Tb.Ar (mm <sup>2</sup> )	16.78 ± 3.66	10.74 ± 3.93	56.2*
Ct.Ar (mm <sup>2</sup> )	37.32 ± 8.31	32.52 ± 4.58	14.8
Ct.Pm (mm <sup>2</sup> )	29.48 ± 3.46	26.62 ± 1.40	10.7*
<b>Volumetric bone density</b>			
Total.vBMD (mg HA/cm <sup>3</sup> )	631.1 ± 62.9	716.6 ± 76.2	- 11.9*
Tb.vBMD (mg HA/cm <sup>3</sup> )	190.0 ± 40.7	199.5 ± 40.4	- 4.8
Ct.vBMD (mg HA/cm <sup>3</sup> )	805.7 ± 66.0	843.9 ± 43.9	- 4.5
<b>Bone microstructure</b>			
Tb.BV/TV	0.29 ± 0.07	0.30 ± 0.06	- 3.3
Tb.N (1/mm)	0.68 ± 0.22	0.67 ± 0.13	1.5
Tb.Th (mm)	0.30 ± 0.05	0.30 ± 0.03	0
Tb.Sp (mm)	1.40 (1.14~1.63)	1.10 (0.87~1.17)	27.3*
Ct.Th (mm)	2.03 ± 0.44	1.94 ± 0.39	4.6
Ct.Po (%)	2.50 (1.80~3.40)	2.80 (1.90~4.70)	- 10.7
<b>Bone biomechanical indices</b>			
CSMI (mm <sup>4</sup> )	257.4 ± 98.5	185.0 ± 52.9	39.1*
BSI (mm <sup>4</sup> /mg HA/cm <sup>3</sup> )	210124 ± 84662	154741 ± 43412	35.8

Tb.Sp and Ct.Po were expressed as medians interquartile range. The remaining index value was mean ± SD

*Total.Ar* total area, *Tb.Ar* trabecular area, *Ct.Ar* cortical area, *Ct.Pm* cortical perimeter, *Total.vBMD* total volumetric bone mineral density, *Tb.vBMD* trabecular volumetric bone mineral density, *Ct.vBMD* cortical volumetric bone mineral density, *Tb.BV/TV* trabecular bone fraction, *Tb.N* trabecular number, *Tb.Th* trabecular thickness, *Tb.Sp* trabecular separation, *Ct.Th* cortical thickness, *Ct.Po* cortical porosity, *CSMI* cross-sectional moment of inertia, *BSI* bone strength index

\*Significantly different from the controls, data italicized if  $p \leq 0.05$

## Discussion

This study was designed to investigate bone microarchitecture at distal interphalangeal joints in PHO patients by HR-pQCT, including evaluation of bone geometry, volumetric density (vBMD), microstructure parameters, and bone erosions at the 3rd DIPs. Bone cross-areas and reduced total vBMD were found in PHO patients than healthy controls. The parameters reflecting bone microstructure were not significantly different between the patients and controls except the trabecular separation which was greater in PHO patients. Compared with X-ray examination, HR-pQCT assessment on bone erosions at the 3rd DIP was more sensitive. Our study firstly evaluated the ability of HR-pQCT to detect and compare the differences of the bone microstructure at DIPs between PHO patients and healthy controls. Our findings on the erosions at finger joints detected by HR-pQCT in PHO patients provide evidence for the further study on PHO pathogenic identification associated bone damage and joint impairment.

To date, over 100 patients with PHO have been reported in all published PHO studies [2–4, 9–12, 27–31]. Only two of the reported cases were female as the atypical features of

female PHO patients with less skin and skeletal symptoms [27, 28]. The 15 PHO patients recruited in our current study were all male. The most frequent triads of these PHO patients were pachydermia, distal clubbing, hyperhidrosis, and periostosis which matched to the features reported previously. Besides, about seven of the 15 PHO patients presented with hand pain, while only two of them had swelling of the affected hand. Pain and swelling in hands were the common symptoms in all forms of arthritis. A previous study indicated that individuals with erosive hand arthritis disease experienced more pain than individuals with nonerosive hand arthritis disease [32]. This finding implied that the erosion might be one of the reasons causing pain. Conventional radiography was considerate as the gold standard for bone erosion diagnosis in articular cartilage disease [16, 32]. Diagnosis of erosion was based on central erosions and collapse of the subchondral bone plate on radiographs in interphalangeal joints [32]. However, previous plain radiographic studies of PHO patients only showed acro-osteolysis at distal phalangeal, and few studies described bone erosions in interphalangeal joints [4, 28]. To detect bone erosions in hands, bone erosions of each DIP and PIP joint were evaluated by using grading score of

**Table 4** Biochemical markers in PHO patients and healthy controls

	PHO patients ( <i>n</i> = 15)	Healthy controls ( <i>n</i> = 12)	<i>P</i> value
Serum PGE <sub>2</sub> (pg/ml)	328.2 (175.7~2576)*	169.1 (28.71~299.9)	0.001
Proinflammatory cytokines			
hsCRP (mg/L)	20.2 ± 23.3*	0.50 ± 0.38	0.008
ESR (mmg/h)	15.5 ± 11.1*	4.17 ± 1.64	0.002
TNF-α (pg/ml)	8.92 ± 3.18*	5.53 ± 1.39	0.002
IL-6 (pg/ml)	6.75 ± 6.96*	2.94 ± 1.10	0.037
Bone metabolic markers			
iPTH (pg/ml)	43.7 ± 18.9	37.3 ± 13.3	0.337
ALP (U/L)	92.7 ± 26.3	82.8 ± 12.5	0.241
β-CTX (ng/ml)	0.93 ± 0.42*	0.40 ± 0.06	0.0002
Free sRANKL/OPG	279.3 ± 178.2*	132.9 ± 72.11	0.013
Cartilage degeneration markers			
MMP1 (pg/ml)	1182 ± 184.3*	549.1 ± 156.8	0.020
MMP13 (pg/ml)	804.9 ± 183.7	538.5 ± 94.29	0.277

The level of serum PGE<sub>2</sub> was expressed as medians interquartile range. The remaining biomarkers value were presented as mean ± SD

*hsCRP* hypersensitive C reactive protein, *ESR* erythrocyte sedimentation rate, *TNF-α* tumor necrosis factor alpha, *IL-6* interleukin 6, *iPTH* intact parathyroid hormone, *ALP* alkaline phosphatase, *β-CTX* beta-C-telopeptides of type I collagen, *Free sRANKL/OPG* the ratio of free soluble receptor activator of nuclear factor-kappa B Ligand to osteoprotegerin, *MMP1* metalloproteinase-1, *MMP13* metalloproteinase-13

\*Significantly different from the controls, data italicized if  $p \leq 0.05$

Atlas of Standard Radiographs of Arthritis based on X-ray images [20]. The results showed that hand bone erosions presented in ten PHO patients and the 3rd DIP were the most frequently affected interphalangeal joint. The medical records of these 15 PHO patients were reviewed and found that two of the patients have suffered pain for about 1 year without diagnosis of erosion in hands [33, 34]. This might be due to the relatively low sensitivity of X-ray in detection of bone erosions in the early phase of the disease. We thereby used more sensitive radiographic technique, HR-pQCT, to measure bone erosions in PHO patients. In the present study, the 3rd DIP was defined as the ROI and erosion size was measured based on the HR-pQCT images. Based on HR-pQCT images, bone erosions were found in 14 PHO patients and three healthy controls at the 3rd DIP, which was more sensitive compared to X-ray screening (Fig. 1). Furthermore, the average size of depth, width, and volume of erosions in PHO patients were all < 2 mm, indicating that PHO patients were in the early stage of arthritis disease and had articular damage in the interphalangeal joint [19, 32].

Articular bone erosion was considered as localized osteolysis (bone loss) involving in cortical bone, and damaging of the normal barrier between the extraskelatal tissue and intertrabecular space of the bone marrow cavity [33]. It was noted that Gruneboom et al. [35] have recently discovered that thousands of blood vessels traversed perpendicularly across the cortical bone. Therefore, the erosions might also be the transcortical blood vessels. HR-pQCT has a higher sensitivity

than the conventional plain X-ray to detect cortical interruptions in finger joints [36]. However, it appeared that HR-pQCT imaging was still insufficient to delineate vascular channels (VC) erosions. Scharnaga et al. [36] have studied the VC in metacarpophalangeal joints by using both HR-pQCT and histologic sectioning. They found that 75% of VC identified by histology was classified as a cortical interruption or periosteal excavation on matched single HR-pQCT slice [36]. Thus, to correctly assess the erosions of PHO patient's, diagnosis should be driven by the combination of HR-pQCT and histological analysis to avoid the influence of vascular vessels. As biopsy from PHO patients was not available in the present study, the histopathological assessments were not able to be conducted.

HR-pQCT assessment allowed a detailed evaluation of bone geometry, vBMD, bone microstructure, and non-invasive bone strength in order to advance understand and compare the skeletal pathophysiology of PHO patients and healthy controls. Therefore, in this study, the Total.Ar, Tb.Ar, and Ct.Pm in the cross-sectional ROI of 3rd DIP were distinctly higher than that of the controls, while Ct.Ar of PHO patients was comparable to the controls. These findings were consistent to results reported in the previous studies by using X-ray radiographs, which showed typical subperiosteal new bone formation in the distal phalangeal, or other distal parts of radius, tibia metacarpals, and metatarsals [2–4, 10]. Despite of new bone formation taking place in the distal phalangeal, the total vBMD (− 11.9%,  $p < 0.05$ ) was found lower in PHO

**Table 5** Correlations of HR-pQCT parameters with proinflammatory markers (*r*)

	Serum PGE2	hsCRP	ESR	IL-6	TNF- $\alpha$
Total.Ar (mm <sup>2</sup> )	0.3791	- 0.2662	0.1147	0.4160	- 0.0806
Tb.Ar (mm <sup>2</sup> )	0.5198	0.2039	<b>0.5556*</b>	0.1419	- 0.0828
Ct.Ar (mm <sup>2</sup> )	0.1560	- 0.3786	- 0.1932	0.3709	0.2503
Ct.Pm (mm <sup>2</sup> )	0.2879	- 0.3950	- 0.1280	0.2925	0.1171
Total.vBMD (mg HA/cm <sup>3</sup> )	<b>- 0.5440*</b>	<b>- 0.5824*</b>	<b>- 0.5683*</b>	- 0.1470	0.1751
Tb.vBMD (mg HA/cm <sup>3</sup> )	0.1122	0.1573	- 0.0555	- 0.3619	- 0.2366
Ct.vBMD (mg HA/cm <sup>3</sup> )	- 0.3934	- 0.3571	- 0.1789	- 0.0247	- 0.2283
Tb.BV/TV	0.1341	0.0964	0.1413	- 0.2180	- 0.3851
Tb.N (1/mm)	0.2176	0.1286	0.2665	- 0.2810	- 0.2256
Tb.Th (mm)	0.2112	- 0.0232	- 0.2453	- 0.1191	0.1080
Tb.Sp (mm)	0.1045	- 0.0264	0.1069	0.3113	0.1296
Ct.Th (mm)	- 0.1516	- 0.0536	- 0.0143	0.5057	0.3576
Ct.Po (%)	0.0813	- 0.1466	0.0170	0.4725	0.4821
CSMI (mm <sup>4</sup> )	- 0.3363	<b>- 0.4989*</b>	- 0.2683	0.2855	0.3769
BSI (mm <sup>4</sup> /mg HA/cm <sup>3</sup> )	- 0.3670	<b>- 0.5121*</b>	- 0.2809	0.2405	0.2503

*Total.Ar* total area, *Tb.Ar* trabecular area, *Ct.Ar* cortical area, *Ct.Pm* cortical perimeter, *Total.vBMD* total volumetric bone mineral density, *Tb.vBMD* trabecular volumetric bone mineral density, *Ct.vBMD* cortical volumetric bone mineral density, *Tb.BV/TV* trabecular bone fraction, *Tb.N* trabecular number, *Tb.Th* trabecular thickness, *Tb.Sp* trabecular separation, *Ct.Th* cortical thickness, *Ct.Po* cortical porosity, *CSMI* cross-sectional moment of inertia, *BSI* bone strength index, *hsCRP* hypersensitive C reactive protein, *ESR* erythrocyte sedimentation rate, *TNF- $\alpha$*  tumor necrosis factor alpha, *IL-6* interleukin 6

\*Significant correlation,  $p \leq 0.05$  and indicated in bold

patients than healthy controls, indicating that the mechanical properties of the whole bone of the 3rd DIP could be inferior in PHO patients. To better understand whether there was the biomechanical response of the bones on the 3<sup>rd</sup> DIP in PHO patients, bone strength indices including CSMI and BSI were analyzed in this study. CSMI, which was obtained from bone density and geometric models, has been reported as a biomechanical indicator of the structural distribution of bone mass [37]. Also, BSI was derived from the cortical vBMD and CSMI serves as an important index for predicting bone bending strength [38]. It was found that CSMI in PHO patients was greater than that of healthy controls, whereas there was no significant difference found in BSI between the two groups. The significant lower vBMD of PHO patients might be biomechanically compensated by the enhanced Total.Ar and CSMI, but the enlarged trabecular separation (+ 27.3%,  $p < 0.05$ ) of PHO patients impaired the bone microstructure and might somewhat lesser the function of this compensation. Therefore, there was no significant difference in BSI between the two groups despite of greater CSMI found in PHO patients than the healthy controls. Besides, to clarify whether the lower vBMD was influenced by the geometric indicator of cortical bone of the PHO patients that could support above explanation, we investigated the correlations among geometric indices Ct.Ar, Ct.Th, and CSMI with cortical vBMD. However, due to the small sample size of PHO patients recruited in this study, no significant correlation was revealed between the cortical vBMD and any of the cortical geometric parameters.

In addition, Ke et al. [39] have revealed that *in vivo* PGE2 administration stimulated bone modeling by producing new woven trabeculae. Compared to the lamellar bone with sheet-like structure and stronger mechanical properties, the woven bone was weaker with numbers of randomly but quickly formed oriented collagen fibers [40]. Thus, the larger portion of woven bone in PHO patients might be another reason for cross-sectional bone area enlargement and larger CSMI in 3rd DIP with higher vBMD. Lamellar bone and woven bone could be identified histologically in the future study.

PGE2 could promote osteoclast activity and osteoclastogenesis through inhibiting OPG secretion, stimulating RANKL production and up-regulating RANKL expression [41]. Additionally, inflammation of the bone microenvironment induced both stimulation of bone resorption and suppression of bone formation which contributed to the osteolysis in inflammatory articular disease [42]. Previous studies have demonstrated that enhanced expression of inflammatory cytokines, such as TNF- $\alpha$ , imbalanced bone metabolism by fostering the differentiation of osteoclasts and hampering the formation of osteoblasts [13, 43]. Moreover, IL-6 was increased and associated with the increased bone resorption markers including  $\beta$ -CTX and urinary hydroxyproline/creatinine ratio in PHO patients suggesting that IL-6 mediated osteoclast activity in PHO [11]. In this study, the inflammatory condition in PHO patients was implied by the increasing levels of pro-inflammatory cytokines including hsCRP, ESR, TNF- $\alpha$ , and IL-6. Therefore, apart from the disorganized and weaker woven bone formation, the enhanced



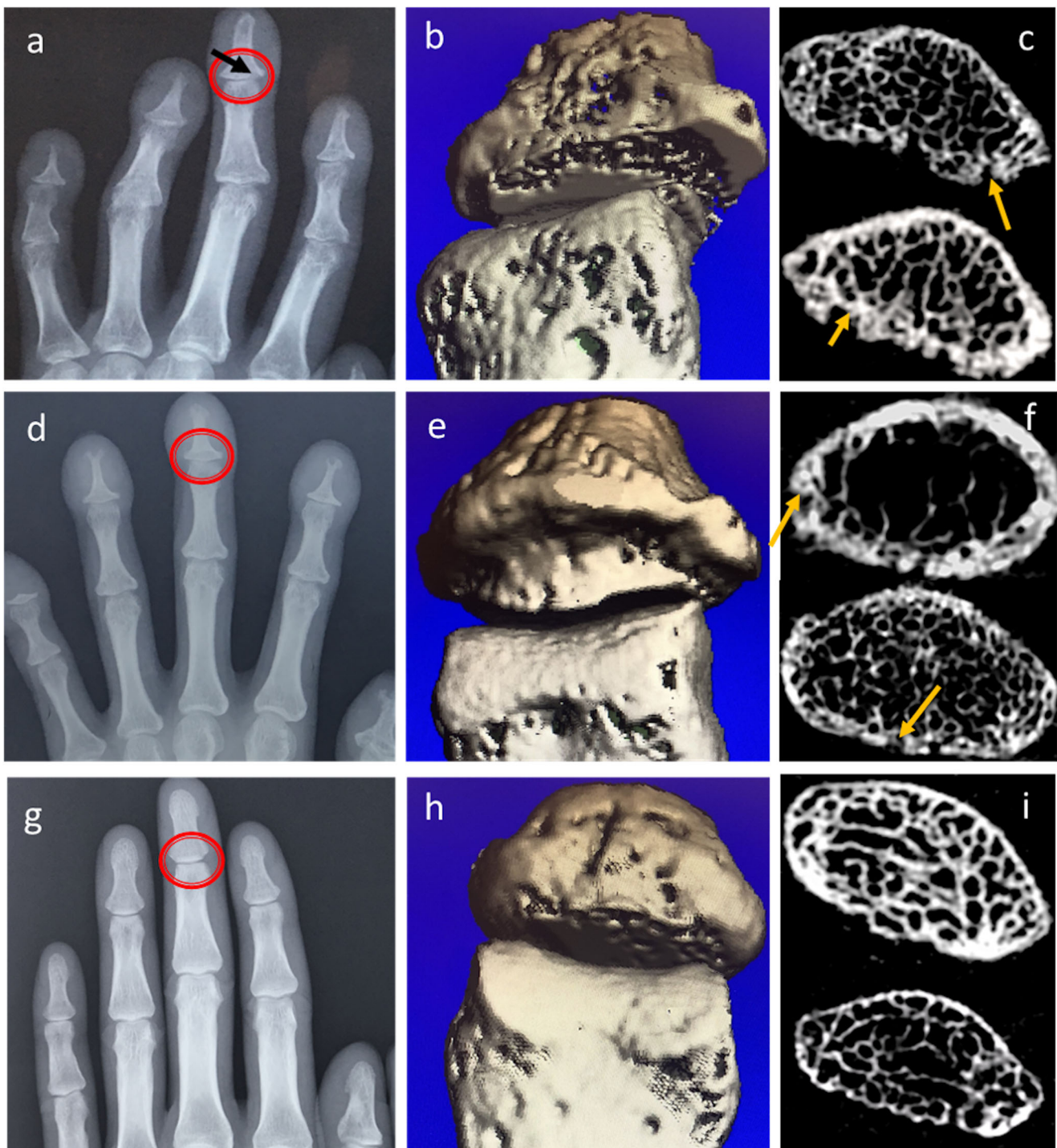


**Fig. 1** The images of 3rd DIP in PHO patients and the healthy controls by X-ray and HR-pQCT. **a–c** Bone erosions of a PHO patient were both observed in X-ray and HR-pQCT image assessment. **d–f** Bone erosions of a PHO patient were only detected in HR-pQCT image evaluation. **g–i**

Healthy controls with no bone erosion seen on X-ray or HR-pQCT. Red circle showed target evaluation region. Black arrow showed erosions on X-ray. Orange arrow showed erosions on HR-pQCT

osteoclasts activity might be another factor in association with the reduction of total  $v$ BMD of PHO patients. In the current study, the significantly higher levels of serum PGE2 levels, inflammatory cytokines, and bone resorption markers were found in PHO patients which suggested that the osteoclast activity was

enhanced. To determine the effect of biological changes on bone morphometry at the DIP sites in PHO patients, we investigated the correlation among bone geometry,  $v$ BMD, microstructure impairment, bone strength, and biochemical markers in PHO patients. Although IL-6, TNF- $\alpha$ ,  $\beta$ -CTX, and free sRANKL/

OPG did not significantly correlate the HR-pQCT parameters, significant negative correlation was found in total vBMD, CSMI, and BSI as compared with serum markers, including PGE2, hsCRP, and ESR, indicating that the higher PGE2 values and pro-inflammatory cytokine levels including hsCRP and ESR in PHO patients negatively impaired their vBMD and bone strength. These results were in line with the published DXA study that reported a significant correlation between hand bone loss and values of ESR and hsCRP [44].

Besides, evidences have also revealed the persistent inflammation at joint, especially the elevated cytokines TNF- $\alpha$ , IL-1, and IL-6, which could contribute to joint degeneration in various articular disease, such as rheumatoid, psoriatic, juvenile, and idiopathic disease [43]. To confirm if there was joint degeneration due to persistent inflammation conditions in PHO patients, the serum joint degeneration biomarkers include MMP1 and MMP13 in both PHO patients, and healthy controls were analyzed. Expectedly, the serum levels of MMP1 and MMP13 were both higher in PHO patients. While probably due to the small sample size, there was no significant difference in MMP13 between the two groups. These results initially confirmed the progression of joint damage in PHO patients.

There were some limitations in our study. Firstly, although more erosions were found in finger joints of PHO patients on HR-pQCT versus plain radiographs, the progress of the disease monitored by HR-pQCT was not performed in this study due to the lower rates of a return visit of the PHO patients. Secondly, unlike volumetric density of the bone directly measured by HR-pQCT, the areal BMD (in grams per square centimeter) assessed by DXA is not the actual mineral density but rather a representation of a combination of bone size and volumetric density. Moreover, DAX measurement was unable to separate cortical bone from trabecular bone [45]. Therefore, the direct comparison between areal and volumetric BMD at distal phalangeal was confounded that resulted in no DXA measurement included in the current study. Thirdly, only serum or plasma inflammation cytokines and joint degeneration biomarkers were measured in the current study, but not the joint synovium fluid which was more sensitive and accurate to define the fate of articular cartilage in PHO study. Further study would be focused on the synovium investigations on the joint damage progression in PHO patients. Last but not least, due to the rare case of PHO, the current study has not recruited the positive control group with treatment of COX-2 selective inhibitor etoricoxib, which was revealed to alleviate the symptoms of PHO including pachydermia, hyperhidrosis, joint swelling, and joint pain, and also reduce the ESR and hsCRP level [4] whether the treatment of etoricoxib could improve the bone density, structure, and repair the bone erosion in PHO patients is still unclear. Further research is needed to clarify this issue.

## Summary

In conclusion, this was the first study to employ HR-pQCT to evaluate bone geometry, vBMD, and bone microstructure at DIPs in PHO patients. Based on the HR-pQCT images, we confirmed that HR-pQCT was more sensitive in detecting erosions at the 3rd DIPs in PHO patients compared with traditional radiographs. This study provided solid evidence for application of the HR-pQCT in PHO diagnosis, especially in the early phase of the disease.

**Acknowledgments** We would like to give the sincere thanks to the subjects for consenting to participate in this study.

**Authors' contribution** Prof. Ling Qin and Prof. Weibo Xia were responsible for study design. Ms. Qianqian Pang performed the study and prepared the first draft of the paper. Ms. Qianqian Pang, Dr. Ruoxi Liao, Ms. Yuping Xu, Ms. Yanfang Hou, and Dr. Jiankun Xu contributed to the clinical and experimental work. Dr. Vivian W Hung, Dr. Xuan Qi, and Ms. Qianqian Pang contributed to the imaging analyses. Ms. Qianqian Pang, Dr. Xuan Qi, and Dr. Le Huang were responsible for statistical analysis of the data. All of the authors contributed to revise the paper critically for intellectual content and approved the final version of the submitted manuscript.

**Funding information** This study was supported by the National Natural Science Foundation of China (No.81471088 and No. 81670714) and Bone Quality and Health Assessment Center of the Department of Orthopaedics and Traumatology, the Chinese University of Hong Kong for providing hand fixator for HR-pQCT scanning.

**Compliance with ethical standards** All subjects signed informed consent for imaging measures as well as blood sample collections. This study was approved by the Ethics Committee of PUMCH with the ethics audit number zs-1115.

**Conflicts of interest** None.

## References

- Zhang Z, Zhang C, Zhang Z (2013) Primary hypertrophic osteoarthropathy: an update. *Front Med* 7:60–64
- Uppal S, Diggle CP, Carr IM, Fishwick CW, Ahmed M, Ibrahim GH, Helliwell PS, Latos-Bielenska A, Phillips SE, Markham AF, Bennett CP, Bonthron DT (2008) Mutations in 15-hydroxyprostaglandin dehydrogenase cause primary hypertrophic osteoarthropathy. *Nat Genet* 40:789–793
- Zhang Z, Xia W, He J, Zhang Z, Ke Y, Yue H, Wang C, Zhang H, Gu J, Hu W, Fu W, Hu Y, Li M, Liu Y (2012) Exome sequencing identifies SLCO2A1 mutations as a cause of primary hypertrophic osteoarthropathy. *Am J Hum Genet* 90:125–132
- Li SS, He JW, Fu WZ, Liu YJ, Hu YQ, Zhang ZL (2017) Clinical, biochemical, and genetic features of 41 Han Chinese families with primary hypertrophic osteoarthropathy, and their therapeutic response to etoricoxib: results from a six-month prospective clinical intervention. *J Bone Miner Res* 32:1659–1666
- Yap FY, Skalski MR, Patel DB, Schein AJ, White EA, Tomasian A, Masih S, Matcuk GJ (2017) Hypertrophic osteoarthropathy: clinical and imaging features. *Radiographics* 37:157–195

6. Diggle CP, Carr IM, Zitt E, Wusik K, Hopkin RJ, Prada CE, Calabrese O, Rittinger O, Punaro MG, Markham AF, Bonthron DT (2010) Common and recurrent HPGD mutations in Caucasian individuals with primary hypertrophic osteoarthropathy. *Rheumatology* 49(6):1056–1062
7. Li X, Ellman M, Muddasani P, Wang JH, Cs-Szabo G, van Wijnen AJ, Im HJ (2009) Prostaglandin E2 and its cognate EP receptors control human adult articular cartilage homeostasis and are linked to the pathophysiology of osteoarthritis. *Arthritis Rheum* 60:513–523
8. McCoy JM, Wicks JR, Audoly LP (2002) The role of prostaglandin E2 receptors in the pathogenesis of rheumatoid arthritis. *J Clin Invest* 110:651–658
9. Ricciotti E, FitzGerald GA (2011) Prostaglandins and inflammation. *Arterioscler Thromb Vasc Biol* 31:986–1000
10. Hou Y, Lin Y, Qi X, Yuan L, Liao R, Pang Q, Cui L, Jiang Y, Wang O, Li M, Dong J, Xia W (2018) Identification of mutations in the prostaglandin transporter gene *SLCO2A1* and phenotypic comparison between two subtypes of primary hypertrophic osteoarthropathy (PHO): A single-center study. *Bone* 106:96–102
11. Rendina D, De Filippo G, Viceconti R, Soscia E, Sirignano C, Salvatore M, Della MM, Scaranò G, Mossetti G (2008) Interleukin (IL)-6 and receptor activator of nuclear factor (NF)-kappaB ligand (RANKL) are increased in the serum of a patient with primary pachydermoperiostosis. *Scand J Rheumatol* 37:225–229
12. Adams B, Amin T, Leone V, Wood M, Kraft JK (2016) Primary hypertrophic osteoarthropathy: ultrasound and MRI findings. *Pediatr Radiol* 46:727–730
13. Redlich K, Smolen JS (2012) Inflammatory bone loss: pathogenesis and therapeutic intervention. *Nat Rev Drug Discov* 11:234–250
14. Ejbjerg B, Narvestad E, Rostrup E, Szkudlarek M, Jacobsen S, Thomsen HS, Ostergaard M (2004) Magnetic resonance imaging of wrist and finger joints in healthy subjects occasionally shows changes resembling erosions and synovitis as seen in rheumatoid arthritis. *Arthritis Rheum* 50:1097–1106
15. Geusens P, Chapurlat R, Schett G, Ghasem-Zadeh A, Seeman E, de Jong J, van den Bergh J (2014) High-resolution in vivo imaging of bone and joints: a window to microarchitecture. *Nat Rev Rheumatol* 10:304–313
16. Dohn UM, Ejbjerg BJ, Hasselquist M, Narvestad E, Moller J, Thomsen HS, Ostergaard M (2008) Detection of bone erosions in rheumatoid arthritis wrist joints with magnetic resonance imaging, computed tomography and radiography. *Arthritis Res Ther* 10:R25
17. Regensburger A, Rech J, Englbrecht M, Finzel S, Kraus S, Hecht K, Kleyer A, Haschka J, Hueber AJ, Cavallaro A, Schett G, Faustini F (2015) A comparative analysis of magnetic resonance imaging and high-resolution peripheral quantitative computed tomography of the hand for the detection of erosion repair in rheumatoid arthritis. *Rheumatology (Oxford)* 54:1573–1581
18. Stach CM, Bauerle M, Englbrecht M, Kronke G, Engelke K, Manger B, Schett G (2010) Periarticular bone structure in rheumatoid arthritis patients and healthy individuals assessed by high-resolution computed tomography. *Arthritis Rheum* 62:330–339
19. Fouque-Aubert A, Boutroy S, Marotte H, Vilayphiou N, Bacchetta J, Miossec P, Delmas PD, Chapurlat RD (2010) Assessment of hand bone loss in rheumatoid arthritis by high-resolution peripheral quantitative CT. *Ann Rheum Dis* 69:1671–1676
20. Altman RD, Gold GE (2007) Atlas of individual radiographic features in osteoarthritis, revised. *Osteoarthritis Cartilage* 15(Suppl A):A1–A56
21. Srikhum W, Virayavanich W, Burghardt AJ, Yu A, Link TM, Imboden JB, Li X (2013) Quantitative and semiquantitative bone erosion assessment on high-resolution peripheral quantitative computed tomography in rheumatoid arthritis. *J Rheumatol* 40:408–416
22. Finzel S, Ohrndorf S, Englbrecht M, Stach C, Messerschmidt J, Schett G, Backhaus M (2011) A detailed comparative study of high-resolution ultrasound and micro-computed tomography for detection of arthritic bone erosions. *Arthritis Rheum* 63:1231–1236
23. Yue J, Griffith JF, Xiao F, Shi L, Wang D, Shen J, Wong P, Li EK, Li M, Li TK, Zhu TY, Hung VW, Qin L, Tam LS (2017) Repair of bone erosion in rheumatoid arthritis by denosumab: a high-resolution peripheral quantitative computed tomography study. *Arthritis Care Res* 69:1156–1163
24. Tang XL, Qin L, Kwok AW, Zhu TY, Kun EW, Hung VW, Griffith JF, Leung PC, Li EK, Tam LS (2013) Alterations of bone geometry, density, microarchitecture, and biomechanical properties in systemic lupus erythematosus on long-term glucocorticoid: a case-control study using HR-pQCT. *Osteoporos Int* 24:1817–1826
25. Ding M, Lin XZ, Liu WG (2018) Three-dimensional morphometric properties of rod- and plate-like trabeculae in adolescent cancellous bone. *J Orthop Translat* 12:26–35
26. Zhu TY, Griffith JF, Qin L, Hung VW, Fong TN, Au SK, Tang XL, Kwok AW, Leung PC, Li EK, Tam LS (2013) Structure and strength of the distal radius in female patients with rheumatoid arthritis: a case-control study. *J Bone Miner Res* 28:794–806
27. Zhang Z, He JW, Fu WZ, Zhang CQ, Zhang ZL (2013) Mutations in the *SLCO2A1* gene and primary hypertrophic osteoarthropathy: a clinical and biochemical characterization. *J Clin Endocrinol Metab* 98:E923–E933
28. Yuan L, Chen L, Liao RX, Lin YY, Jiang Y, Wang O, Li M, Xing XP, Pang QQ, Jiajue R, Xia WB (2015) A common mutation and a novel mutation in the HPGD gene in nine patients with primary hypertrophic osteoarthropathy. *Calcif Tissue Int* 97:336–342
29. Erken E, Koroglu C, Yildiz F, Ozer HT, Gulek B, Tolun A (2015) A novel recessive 15-hydroxyprostaglandin dehydrogenase mutation in a family with primary hypertrophic osteoarthropathy. *Mod Rheumatol* 25:315–321
30. Madruga DJ, Rosa RS, Perpetuo I, Rodrigues AM, Janeiro A, Costa MM, Gaiao L, Pereira DSJ, Fonseca JE, Miltenberger-Miltenyi G (2014) Pachydermoperiostosis in an African patient caused by a Chinese/Japanese *SLCO2A1* mutation-case report and review of literature. *Semin Arthritis Rheum* 43:566–569
31. Seifert W, Kuhnisch J, Tuysuz B, Specker C, Brouwers A, Horn D (2012) Mutations in the prostaglandin transporter encoding gene *SLCO2A1* cause primary hypertrophic osteoarthropathy and isolated digital clubbing. *Hum Mutat* 33:660–664
32. Kwok WY, Kloppenburg M, Rosendaal FR, van Meurs JB, Hofman A, Bierma-Zeinstra SM (2011) Erosive hand osteoarthritis: its prevalence and clinical impact in the general population and symptomatic hand osteoarthritis. *Ann Rheum Dis* 70:1238–1242
33. Peters M, van Tubergen A, Scharmga A, Driessen A, van Rietbergen B, Loeffen D, Weijers R, Geusens P, van den Bergh J (2018) Assessment of cortical interruptions in the finger joints of patients with rheumatoid arthritis using HR-pQCT, radiography, and MRI. *J Bone Miner Res* 33:1676–1685
34. Schett G, Gravallesse E (2012) Bone erosion in rheumatoid arthritis: mechanisms, diagnosis and treatment. *Nat Rev Rheumatol* 8:656–664
35. Gruneboom A, Hawwari I, Weidner D, Culemann S, Muller S, Henneberg S, Brenzel A, Merz S, Bornemann L, Zec K, Wuelling M, Kling L, Hasenberg M, Voortmann S, Lang S, Baum W, Ohs A, Kraff O, Quick HH, Jager M, Landgraaber S, Dudda M, Danuser R, Stein JV, Rohde M, Gelse K, Garbe A, Adamczyk A, Westendorf AM, Hoffmann D, Christiansen S, Engel DR, Vorkamp A, Kronke G, Herrmann M, Kamradt T, Schett G, Hasenberg A, Gunzer M (2019) A network of trans-cortical capillaries as mainstay for blood circulation in long bones. *Nat Metab* 1:236–250
36. Scharmga A, Keller KK, Peters M, van Tubergen A, van den Bergh JP, van Rietbergen B, Weijers R, Loeffen D, Hauge EM, Geusens P (2017) Vascular channels in metacarpophalangeal joints: a comparative histologic and high-resolution imaging study. *Sci Rep* 7:8966
37. Siu WS, Qin L, Leung KS (2003) pQCT bone strength index may serve as a better predictor than bone mineral density for long bone breaking strength. *J Bone Miner Metab* 21:316–322

38. Greene D, Naughton G, Briody J, Kemp A, Woodhead H, Corrigan L, Karisson M (2005) Bone strength index in adolescent girls: does physical activity make a difference? *Br J Sports Med* 39:622–627
39. Ke HZ, Jee WS, Mori S, Li XJ, Kimmel DB (1992) Effects of long-term daily administration of prostaglandin-E2 on maintaining elevated proximal tibial metaphyseal cancellous bone mass in male rats. *Calcif Tissue Int* 50:245–252
40. Turner CH, Forwood MR, Rho JY, Yoshikawa T (1994) Mechanical loading thresholds for lamellar and woven bone formation. *J Bone Miner Res* 9:87–97
41. Zhang X, Schwarz EM, Young DA, Puzas JE, Rosier RN, O'Keefe RJ (2002) Cyclooxygenase-2 regulates mesenchymal cell differentiation into the osteoblast lineage and is critically involved in bone repair. *J Clin Invest* 109:1405–1415
42. Visser K, Goekoop-Ruiterman YP, de Vries-Bouwstra JK, Ronda HK, Seys PE, Kerstens PJ, Huizinga TW, Dijkman BA, Allaart CF (2010) A matrix risk model for the prediction of rapid radiographic progression in patients with rheumatoid arthritis receiving different dynamic treatment strategies: post hoc analyses from the BeSt study. *Ann Rheum Dis* 69:1333–1337
43. Finzel S, Rech J, Schmidt S, Engelke K, Englbrecht M, Stach C, Schett G (2011) Repair of bone erosions in rheumatoid arthritis treated with tumour necrosis factor inhibitors is based on bone apposition at the base of the erosion. *Ann Rheum Dis* 70:1587–1593
44. Devlin J, Lilley J, Gough A, Huissoon A, Holder R, Reece R, Perkins P, Emery P (1996) Clinical associations of dual-energy X-ray absorptiometry measurement of hand bone mass in rheumatoid arthritis. *Br J Rheumatol* 35:1256–1262
45. Haapasalo H, Kontulainen S, Sievanen H, Kannus P, Jarvinen M, Vuori I (2000) Exercise-induced bone gain is due to enlargement in bone size without a change in volumetric bone density: a peripheral quantitative computed tomography study of the upper arms of male tennis players. *Bone* 27:351–357

**Publisher's note** Springer Nature remains neutral with regard to jurisdictional claims in published maps and institutional affiliations.

## Affiliations

Q. Pang<sup>1,2</sup> · Y. Xu<sup>1,3</sup> · X. Qi<sup>1</sup> · L. Huang<sup>2</sup> · V.W. Hung<sup>2</sup> · J. Xu<sup>2</sup> · R. Liao<sup>1</sup> · Y. Hou<sup>1</sup> · Y. Jiang<sup>1</sup> · W. Yu<sup>4</sup> · O. Wang<sup>1</sup> · M. Li<sup>1</sup> · X. Xing<sup>1</sup> · W. Xia<sup>1</sup> · L. Qin<sup>2</sup>

<sup>1</sup> Department of Endocrinology, Key Laboratory of Endocrinology, Ministry of Health, Peking Union Medical College Hospital, Chinese Academy of Medical Sciences, Shuaifuyuan No.1, Dongcheng District, Beijing 100730, China

<sup>2</sup> Musculoskeletal Research Laboratory and Bone Quality and Health Assessment Centre, Department of Orthopedics & Traumatology, The Chinese University of Hong Kong, 5/F Lui Che Woo Clinical Sciences Building, Prince of Wales Hospital, Shatin, N.T., Hong Kong, SAR, Hong Kong

<sup>3</sup> Department of Endocrinology, The First Affiliated Hospital of Shanxi Medical University, Taiyuan 030001, Shanxi, China

<sup>4</sup> Department of Radiology, Peking Union Medical College Hospital, Chinese Academy of Medical Sciences, Beijing 100730, China